

Available online at www.sciencedirect.com

ScienceDirect

journal homepage: www.intl.elsevierhealth.com/journals/dema

Properties of a modified quaternary ammonium silane formulation as a potential root canal irrigant in endodontics

Umer Daood^{a,*}, Abhishek Parolia^a, Jukka Matinlinna^b, Cynthia Yiu^c,
Hany Mohamed Aly Ahmed^d, Amr Fawzy^e

^a Division of Clinical Dentistry, School of Dentistry, International Medical University Kuala Lumpur, 126, Jalan Jalil Perkasa 19, Bukit Jalil, 57000 Bukit Jalil, Wilayah Persekutuan Kuala Lumpur, Malaysia

^b Dental Materials Science, Applied Oral Sciences, Faculty of Dentistry, The University of Hong Kong, 34 Hospital Road, Sai Ying Pun, Hong Kong SAR, China

^c Pediatric Dentistry and Orthodontics, Faculty of Dentistry, The University of Hong Kong, Prince Philip Dental Hospital, 34 Hospital Road, Pokfulam, Hong Kong, China Hong Kong Special Administrative Region

^d Department of Restorative Dentistry, Faculty of Dentistry, University of Malaya, 50603, Kuala Lumpur, Malaysia

^e UWA Dental School, University of Western Australia, Nedlands, WA 6009, Australia

ARTICLE INFO

Article history:

Received 1 May 2020

Received in revised form

28 June 2020

Accepted 9 September 2020

Available online xxx

Keywords:

Endodontics

Antimicrobial

K21

β -galactosidase

Silane

ABSTRACT

Objectives. Evaluate a new modified quaternary ammonium silane irrigant solution for its antimicrobial, cytotoxic and mechanical properties of dentine substrate.

Methods. Root canal preparation was performed using stainless steel K-files™ and F4 size protaper with irrigation protocols of 6% NaOCl + 2% CHX; 3.5% QIS; 2% QIS and sterile saline. Biofilms were prepared using *E. faecalis* adjusted and allowed to grow for 3 days, treated with irrigants, and allowed to grow for 7 days. AFM was performed and surface free energy calculated. MC3T3 cells were infected with endo irrigant treated *E. faecalis* biofilms. Raman spectroscopy of biofilms were performed after bacterial re-growth on root dentine and exposed to different irrigation protocols and collagen fibers analysed collagen fibers using TEM. Antimicrobial potency against *E. faecalis* biofilms and cytotoxicity against 3T3 NIH cells were also. Resin penetration and MitoTracker green were also evaluated for sealer penetration and mitochondrial viability. Data were analysed using One-way ANOVA, principal component analysis and post-hoc Fisher's least-significant difference.

Results. Elastic moduli were maintained amongst control (5.5 ± 0.9) and 3.5% QIS (4.4 ± 1.1) specimens with surface free energy higher in QIS specimens. MC3T3 cells showed reduced viability in 6%NaOCl+2%CHX specimens compared to QIS specimens. DNA/purine were expressed in increased intensities in control and 6% NaOCl + 2% CHX specimens with bands around $480\text{--}490\text{ cm}^{-1}$ reduced in QIS specimens. 3.5% QIS specimens showed intact collagen fibrillar network and predominantly dead bacterial cells in confocal microscopy. 3.5% QIS irrigant formed a thin crust-type surface layer with cytoplasmic extensions of 3T3NIH spread over root dentine. Experiments confirmed MitoTracker accumulation in 3.5% treated cells.

* Corresponding author.

E-mail address: umerdaood@imu.edu.my (U. Daood).

<https://doi.org/10.1016/j.dental.2020.09.008>

0109-5641/© 2020 The Academy of Dental Materials. Published by Elsevier Inc. All rights reserved.

Significance. Novel QIS root canal irrigant achieved optimum antimicrobial protection inside the root canals facilitating a toxic effect against the *Enterococcus faecalis* biofilm. Root dentine substrates exhibited optimum mechanical properties and there was viability of fibroblastic mitochondria.

© 2020 The Academy of Dental Materials. Published by Elsevier Inc. All rights reserved.

1. Introduction

The main objective of root canal treatment procedures is to promote healing of apical periodontitis induced by the microorganisms and their toxins [1]. This is either the source of primary infection or associated with failure of secondary or persistent root canal treatments [1]. Complex biofilms are adhered to the intraradicular dentine [2] extending within the root canal system including lateral canals, isthmi and recesses. Residual bacteria survive in these areas putting the entire treatment outcome at risk in the presence of a newly found nutrient supply [3]. The infected root canal can harbor many bacterial species including *Treponema*, *Streptococcus*, *Fusobacterium*, *Porphyromonas* as well as other cultivable species [4]. Interactions of these biofilm community members may result in symptomatic endodontic infections [5] and swelling [6]. *Enterococcus faecalis* (*E. faecalis*) is prevalent in root canal infections, being one of the most common microorganism in intraradicular infections [7], that survive in harsh environments of high alkalinity and it is resistant to many antimicrobial agents [8]. It is difficult to fully eradicate *E. faecalis* bacterium colonised inside the root canal using antimicrobial agents [9]. Due to the emergence of antibiotic resistance for many bacterial species, new disinfection protocols are obviously needed.

The purpose of a root canal treatment is to remove pulp tissues, microorganisms and potential substrate for microbial regrowth [10]. Complete elimination of bacteria and their metabolic by-products have rarely been observed using chemo-mechanical instrumentation and intracanal medications [11]. Traditional non-specific antimicrobials and irrigants appear to be limited in controlling the infection. Dakin's solution, an antiseptic consisting of a dilute solution of sodium hypochlorite (NaOCl), is one of the most important types of chlorine-releasing agents that has been used as primary root canal irrigant as early as the 1920s [12]. In the decomposition reaction, release of chloride ions and oxygen is possible. Because of its prominent antimicrobial properties and ability to dissolve organic tissue remnants [13], NaOCl still remains the most pivotal irrigating solution employed in the contemporary endodontic practice [14]. The tissue-dissolving capability is primarily related to its concentration. The recommended concentration of NaOCl ranges from 0.5% to 6% in the past, with no consensus on the ideal concentration [15]. Apart from its tissue dissolution properties, NaOCl has deleterious effects on the mineralised dentine canal wall, damaging the dentine integrity [16]. Previous studies have pointed out changes in the composition of dentine with exposure to NaOCl irrigation protocols during root canal therapy [17] reducing the mechanical properties (strength) of dentine predispos-

ing teeth to fracture [18]. Moreover, NaOCl irrigant solution is also known for its hypersensitivity or allergic reactions [19] including palatal tissue necrosis [20], lip burning and diffuse pain [21], which have been reported in the literature as complications caused by the inadvertent handling of NaOCl. With the use of NaOCl and chlorhexidine (CHX) as irrigants, a brownish-orange precipitate is formed commonly known as parachloroaniline (PCA). This primarily causes discolouration [22] and subsequent resistance to free flow of resin material due to blockage of laterals canals causing inadequate sealing of obturating materials [23]. Hence, there is a constant need to find effective but also safe irrigating solutions which display excellent antimicrobial properties and good biocompatibility with the surrounding tissue.

Silanes are synthetic inorganic-organic hybrid C-Si compounds used in numerous dental applications [24]. A quaternary ammonium silane (QAS; codenamed K21; C92H204Cl4N4O12Si5; CAS number 1566577-36-3) was synthesized using the sol-gel reaction, by allowing tetraethoxysilane to react as the anchoring unit and 3-(triethoxysilyl)propyldimethyloctadecyl ammonium chloride using a molar ratio of 1:4 [25-27]. This promising class of contact-killing antibacterial has a broad spectrum and low toxicity [28]. The antimicrobial activity is attributed to its long, lipophilic -C18H37 alkyl chain penetrating the bacterial membranes causing autolysis and cell death [29]. The quaternary ammonium silane is covalently grafted via Si-O-Si linkages due to the presence of silanol groups [30]. The presence of tetraethoxysilane (TEOS), enables a three-dimensional network comprised of silicate units with condensation of tetra and tri-ethoxysilane species with remaining silanol (-Si-OH) groups [31]. When applied to acid etched dentine, this silicate network condenses within the dentinal substrate providing a long term antimicrobial effect. In general, such compounds have positively charged nitrogen atoms in their lipophilic chemical structures, making them favourable to be taken by mitochondria inhibiting mitochondrial oxidative phosphorylation at low concentrations [32]. Mitochondrial dysfunction by inhibition of oxidative phosphorylation via quaternary ammonium toxicity is a known process causing cell apoptosis [33]. Bacterial infection can enhance apoptosis of osteoblastic cells promote programmed osteoblast death with fate decided between the interaction of pro and anti-apoptotic proteins [34]. *E. faecalis* is known to also survive in harsh environments possessing complicated virulence factors such as lipoteichoic acid (LTA) and gelatinase, enabling its strong pathogenicity [35].

This antimicrobial irrigation system was inspired by our previous work to formulate a new endodontic irrigant, as its function as an irrigant against the traditional NaOCl irrigants was still unknown. One of the most promising novel

approaches to overcome endodontic infections was to use QAS as reported by Daood et al. [27]. Therefore, in this study, as a potential determinant, it was hypothesized that the incorporation of QIS (Quaternary Ammonium Silane Irrigant Solution) as a pure endodontic irrigant, and not as a mixture with NaOCl, can bring significant and safe changes in endodontics. In addition, other effects such as antibacterial potency, cytotoxicity effect of QAS, its potential to reduce apoptosis and mitochondrial effect were evaluated along with an extensive study of *E. faecalis* biofilms. The null hypothesis tested in the present laboratory study was that there is no difference in antibacterial properties of QIS used as a potential endodontic irrigant when compared to other potent solutions (NaOCl, NaOCl + CHX).

2. Materials and methods

Extracted human mandibular third molars ($n = 120$) with fused roots (mesiobuccal canal attempted) and extracted non-carious single rooted anterior teeth ($n = 90$) were collected after attaining patient's informed consent. The teeth chosen had complete root formation, were sound with no carious lesion. Teeth collection was approved by the Institutional Review Board of International Medical University Kuala Lumpur and stored in 0.5% Chloramine-T solution for 3 weeks and then in distilled water at 4 °C until use. All soft tissues around the teeth were removed by immersing the teeth in 5% hydrogen peroxide and gently removing any remains using spoon shaped excavators before use. Unless stated otherwise, the disinfectant solution is provided by FiteBac Kimmerling Holdings Group, LLC (KHG).

2.1. Synthesis of 3.5% QAS/k21 Endo irrigant QAS/k21 endo irrigant

The k21 silane endodontic dispersions were prepared by appropriately diluting the as received k21 [(QAS(k21); KHG FiteBac® Technology, Marietta, GA, USA)] organosilane in absolute ethanol (99.6%) to achieve 3.5% concentration (adjusting with absolute ethanol). A 3.5% concentration was selected after prior string of results using different concentrations of QAS/k21 disinfectant on *E. faecalis* biofilms and observing effect on extracted dental pulp tissue in-vitro (data not shown). Next, 0.3 ml NaOH (M_r 39.997 g/mol = 0.025 m/l) and 0.3 ml EDTA (M_r 292.24 g/mol = 0.003 mol/l \times 3 times) as a disodium salt were blended with 0.75 mg of alexidine (a bisbiguanide). The pH of the dispersions was adjusted with 1.0 M acetic acid solution or potassium hydroxide in a 100 ml round bottom flask. The mixture above was blended with dispersions for at least 10 min to co-disperse all ingredients to produce an even mix with 3.5% k21 silane under inert environment. The k21 silane dispersion was then added slowly with 0.75 mg DDAB, dimethyldioctadecylammonium (M_r 631 g/mol; $C_{38}H_{80}NBr$), further immersed in a glass tubings set up at 30 °C. The reaction mixture was further stirred for 2 h. The solution was kept for 2 h in a sealed vial at ambient temperature. The solution was finally filtered with a target pH ranging between 5-6.5 (details unprovided). The Raman spectroscopy analysis revealed presence of water, ethanol and

all-important silanol groups. Open Si-O-Si cyclic species are identified similar to the QAS disinfectant previously used (Fig. 1A-B).

2.2. Tooth preparation

After cleaning teeth using periodontal cures, and rinsing with sterile saline, the teeth were mounted on an isomet cutting machine (Buehler IsoMet Low Speed, Lake Bluff, IL, USA) under water cooling to remove the occlusal crown completely from just below the cemento-enamel junction to obtain the roots of teeth.

3. The irrigation protocol

Root canal procedures were performed by a trained endodontist (Senior Consultant Faculty) using stainless steel K-files (no. 10-15-20) (Dentsply Sirona, Tulsa Dental, USA) canals for shaping the canals using watch wind motion. Protaper™ rotary file system (Dentsply Maillefer, Ballagues, Switzerland) was used up to file size F4 at a speed of 300 RPM. The working length was kept 1 mm short in the entire procedure in all samples length equal to 11 mm. Crown down technique was performed using #2 and #3 gates glidden drills (Dentsply Maillefer, Ballagues, Switzerland) with apical portion prepared using #35 file (as master apical file). Irrigation was performed using 2 ml of 6% NaOCl (Calasept, Upplands Väsby, Sweden) after each use. Next 6% NaOCl (2 ml) and 17% (2 ml) EDTA (Pulpdent Corporation, Warwick, UK) were used for 2 min. enabling removal of inorganic smear layer and subsequently rinsed with sterile saline. After autoclaving (121 °C, 15 lbs psi), all teeth were randomly divided to one of the following irrigation protocols of 2.5 ml each ($n = 5$): Group A: 6% NaOCl; Group B: 6% NaOCl + 2% CHX; Group C: 3.5% QIS; Group D: 2% QIS and Group E: Sterile Saline. (Ultrasonic agitation was performed for all groups (VDW Ultra, VDW GmbH, Munich, Germany; tip set of E8 for 30 s).

3.1. Biofilm preparation

For biofilm formation, *E. faecalis* (ATCC 29212™) was used in Brain Heart Infusion broth (BHI; Difco Laboratories, Detroit, MI, USA) and adjusted at the 1.5 McFarland turbidity standard. Bacteria were cultured on blood agar plates at 37 °C for 20 h anaerobically. The bacterium was then transferred in brain heart infusion (BHI) broth supplemented with 8% sucrose (pH 7.4) and a minimal amount of xylitol (0-2%) at 37 °C for 48 h. The cells were then centrifuged at 4000 rpm for 15 min and cell pellets washed three times with phosphate buffered solution (PBS, 0.01 M, pH 7.2). The cells were suspended in 100 ml of the growth medium and adjusted to a concentration of McFarland standard no. 3 (109 cells/mL). Using sterilizing syringes, 5 ml of BHI broth and bacterial inoculum were used to fill the canals and allowed to react for 3 days. After 3 days, the irrigation protocol was performed and the bacteria allowed to grow for 7 more days. After 7 days, each tooth was dried with sterile paper points under aseptic conditions. Parallel grooves (2) were made on external surfaces across the mesio-distal direc-

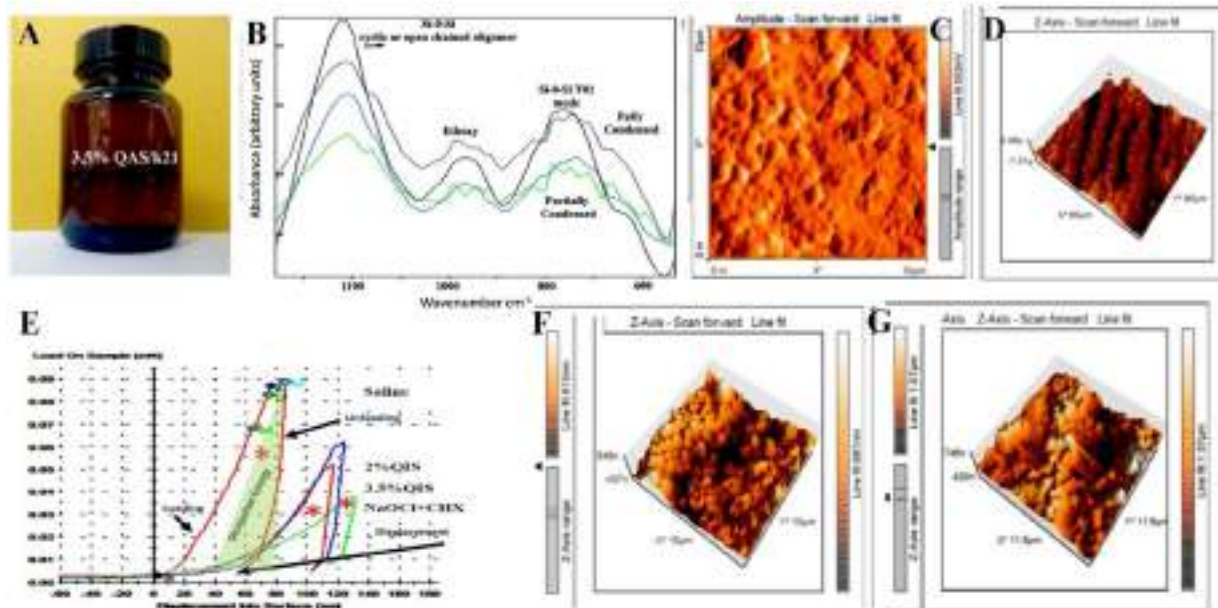


Fig. 1 – Chemical and mechanical AFM characterizations of 3.5% QIS, and QIS treated biofilms on dentine. (A) Sample photo of the aqueous 3.5% QIS irrigant solution; (B) Raman spectroscopy of hydrolysis reaction with spectrum of ethanol as the reference during the sol-gel process; comparative AFM images among the (C) control biofilms specimens treated with saline (D) and 3.5% QIS treated biofilm specimen; (E) load/unload-displacement curves of nanoindentation tests at room temperature under a max load of 1000 mN on different groups and with a scan rate of 0.1 to 0.5 Hz with a retraction speed of 2 $\mu\text{m/s}$. Indentation load function after depth profiling of elastic modulus (extension stretch identified by *) for ultrasonic groups showing differences for experimental groups (*). (F) 3D aspect of 2% QIS and (G) NaOCl + CHX specimens.

tion facilitating a split fracture performed by one operator only. Roots were then separated using a chisel and a hammer and teeth taken for scanning electron microscopy (SEM), confocal laser scanning microscopy (CLSM) and Raman analyses.

3.2. AFM instrumentation

A nano wizard II atomic force microscope (JPK Instruments, Berlin, Germany) with CSC38/NO AL (Mikromasch, Tallinn) probe and cantilever B was used: resonance frequency, 10 kHz, cone with a full cone angle of 40°, force constant, 0.03 N/m, and thickness, 1.0 m. The cantilevers were previously washed with sterile MilliQ water as all AFM procedures were performed at room temperature. AFM imaging was performed using the contact mode with a scan rate of 0.1 to 0.5 Hz with a retraction speed of 2 $\mu\text{m/s}$. The Young's modulus was used to quantify the stiffness of the sample.

3.3. Surface free energy

With each irrigation protocols, 4 mm dentine blocks were obtained by horizontally sectioning below cemento-enamel junction (1 mm) for each group. After splitting the blocks into semi-cylindrical halves, different irrigant formulations were applied in the form of a drop (2 μL) and profile recorded using contact angle analyzer (Dental Simulation Lab, IMU Laboratory). The contact angle was calculated using t/Image J software fitting within the contour of the droplet after plac-

ing on the dentine surface. The following Eq. (1) was used to calculate the free surface energy [36]:

$$\gamma_L(1-\cos\theta) = 2[(\gamma_L^D \gamma_S^D)^{0.5} + (\gamma_L^+ \gamma_S^-)^{0.5} + (\gamma_L^- \gamma_S^+)^{0.5}] \quad (1)$$

where L and S subscripts represent different phases, θ and γ are surface tension and contact angle of the reference liquid used. D, + and - represent the Lewis and dispersive phases. All images were captured in 5 min after placement on dentine surface.

3.4. MC3T3 cells infected with Endo irrigant treated *E. Faecalis* biofilms

α -MEM was used with 10% FBS (Invitrogen, Carlsbad, CA, USA) at 37 °C for culturing of mouse osteoblastic MC3T3-E1 cells (ATCC, Manassas, VA, USA) in presence of 5% CO₂ and saturated humidity. *E. faecalis* (ATCC 29212) was cultured in Tryptone Soya Medium (Hardy Diagnostics, Santa Maria, CA, USA). A single colony was picked and grown at 37 °C in their respective medium to get the microbial suspension for experimental conditions. The microbial suspension's turbidity was adjusted to 0.5 McFarland standard. About 10 ml of the microbial suspension was taken in a sterile tube for *E. faecalis* with respective media. The pre-prepared sterilized dentine blocks were aseptically placed into the tubes with the microbial suspension and allowed to grow for 2 days. Fresh microbial broth was replaced on the third day and maintained up to 21 days. All the experiments were performed in an aseptic condition under a BSL II laminar flow hood (Bioair Safemate, Italy).

The mouse osteoblasts cells were grown overnight in 96-well plates at 3.5×10^3 /well to investigate the effects of *E. faecalis* on osteoblasts. The density of osteoblasts was maintained at 8×10^5 /well and incubated with *E. faecalis* at a multiplicity of infection (MOI) of 1,000:1 for 3 h. Once the cells were infected, the cells were treated with 5 mg/mL nisin for 3 h along with 10 μ g/mL of ciprofloxacin. The mouse osteoblastic cells were cultivated for 6, 12, 36 and 48 h and cells centrifuged at 2000 rpm for 10 min. The cells were incubated with CCK-8 solution and optical density measured at 450 nm (triplicates taken) using a microplate reader (Tecan, Reading, UK); while blanking was conducted with the culture supernatant which was untreated.

3.5. Raman spectroscopy of biofilms

After removing the dentine discs from culture plates, the specimens were dried for 20 min at 35 °C and placed on x-y-z-axis-Raman positioning stage on a low fluorescent quartz microscopic slide. Horiba Jobin Yvon LabRam HR800 micro spectrometer (Horiba Jobin Yvon, NJ, USA) was used for spectrum acquisition using a 100x objective: 514.5 nm green laser excitation, 785 nm with argon ion (with spectral resolution 1.6 cm^{-1}), <500 μ W were applied. Dark count correction with noise removal was carried out for all spectra with normalization with spectral peaks calculated with OriginPro 8.5.1 software (Origin Lab, Northampton, MA, USA) and Rayleigh scattering photons blocked with a notch filter that has a spectral range of -120 to 130 rel cm^{-1} , with an ellipsoid measurement of approximately 1.0 μ m. The spatial resolution was maintained with 350 nm and 2.0 μ m in the horizontal plane. Raman peaks were centered around 434 cm^{-1} (stretching vibration of $\nu_2\text{PO}_4$) [37] and 484 cm^{-1} (polysaccharides or carbohydrates) [38] and 1665 cm^{-1} .

Thirty-six spectra from each spectrum were used for spot-to-spot location for calculation of coefficient of variation. The average spot was calculated location-to-location for the sample. The values were determined by using mean and dividing the standard deviation (SD) to the mean and multiplying it by 100. Also the different disinfectant was successfully discriminated using Principle Component Analysis (PCA).

3.6. Transmission electron microscopy of collagen

Root dentine blocks were exposed to different irrigation protocols to simulate the contact of various irrigation solutions. The specimens ($n = 5$) were then thoroughly washed with deionized water and split into halves for TEM sections. To evaluate the root dentine collagen structure after irrigation protocols, each specimen was completely demineralized in 0.1 M formic acid/sodium formate (pH 2.5). The specimens were fixed with Karnovsky's fixative (2.5 wt% glutaraldehyde and 2% paraformaldehyde in 0.1 mol/l cacodylate buffer; pH, 7.3) for 8 h, and post fixed using 1% osmium tetroxide (OsO_4) for 1 h. Next, the specimens were subjected to dehydration using ascending grades of ethanol (75%-100%) with propylene oxide as a transition medium and finally embedded in pure epoxy resin. An ultramicrotome (Leica Microsystems, Inc., Bannockburn, IL, USA) was used to cut 90 nm thick sections of dentine specimens which were examined unstained using 2%

uranyl acetate and lead citrate. The images of sections were taken using JEM-1230 TEM (JEOL, Tokyo, Japan) at 110 kV.

3.7. Confocal analysis and CFU log of *E. Faecalis* biofilms

Live/Dead BacLight bacterial viability (molecular probe #L7012 LIVE/DEAD BacLight stain; Invitrogen) was used to analyse viability of bacteria in single-specie biofilms on dentine was using a confocal light microscope (Fluoview FV 1000, Olympus, Tokyo, Japan). After mixing the stain according to manufacturer's instructions, the biofilm was imaged between 500 and 550 nm with an excitation wavelength of 488 nm and $\times 100$ objective lens for direct observation. Each specimen was examined using bioimageL software (v.2.0. Malmö, Sweden) showing green-red staining based on colour segmentation algorithms in MATLABTM. Percentages for live and dead bacteria were calculated.

E. faecalis biofilms from the root dentin specimens were collected in 1 mL sterile BHI broth at a pH of 7.4 and further incubated for 24 h at 37 °C. A 100 μ L of each broth from different groups was centrifuged (Centrifuge 5430 R; Eppendorf AG, Hamburg Germany) five times in 100 μ L of PBS inside eppendorf tubes (plastibrand micro centrifuge Tube/Z334006; Sigma-Aldrich). Once completed, 5 μ L of each serial diluted sample was played on selective BHI agar plates for incubation for 24 h. The microbial colonies in colony-forming units [CFU/mL] were counted and further converted to log CFU.

3.8. SEM and resin penetration

Randomly selected dentine root canals ($n = 3$) were subjected to different irrigant protocols according to the groups. After making two parallel grooves in the mesio-distal direction, a chisel and hammer was used to create a split fracture. The specimens were then transferred in ascending grades of ethanol (33%, 66%, 85%, 95%, $2 \times 100\%$, for 20 min in each) for dehydration. Later, the specimens were transferred to critical point drying machine (CPD 30, Leica). Two 1 mm slices were cut and polished using 1200 silicon carbide paper for analysis of interface morphology, between resin-based dentine sealer and root dentine. After etching specimens with 35% ortho-phosphoric acid and washed using deionised water for 10 s, specimens were immersed in 5.25% NaOCl solution for 15 min and rinsed under running water for 5 min. Specimens were fixed using osmium tetra oxide and again immersed in ascending grades of ethanol for 20 min. The specimens were air dried, and mounted on stubs for gold sputtering for 120 s under vacuum to analyse in Philips/FEI XL30 FEG at an accelerating voltage of 10 kV.

3.9. Mitotracker

The NIH 3T3 mouse fibroblastic cell lines were cultured in Dulbecco's Modified Eagle's Medium (DMEM; Sigma-Aldrich Corp., St. Louis, MO, USA) with 10% fetal bovine serum (FBS) and 1% penicillin/streptomycin (10,000 U/100 g/mL) inside a humidified incubator with 5%CO₂ incubator at 37 °C. After expanding the cell culture to 80% confluence, the cells were utilized at sixth passage. The cells were seeded on the pulpal

side of dentine discs in 12-well plates ($n = 10$) in an incubator with 5% CO₂ and 98% air at 37 °C. The cells received the irrigant treatments using saturated microbrush for 20 s. The cells were then incubated with 200 nM MitoTracker Green (mitochondria-specific fluorescent dye; CN M7514-San Francisco, USA) for 20 min and analysed using Axiovert microscope (Carl Zeiss) equipped with a Neofluar 100 NA 1.3 objective (488 nm laser, 490 nm excitation wavelength and 516 nm emission wavelength).

4. Statistical analysis

All experiments in this paper were repeated thrice and the results/data were presented as mean \pm standard deviation (SD) using SPSS 20.0. The expression $p < 0.05$ stand for statistically significant, $**p < 0.01$ for very significant and $***p < 0.001$ for extremely significant values, respectively. The microbiological (percentage of live and dead bacteria) and mechanical property (young's modulus) experiments were analysed using One-way ANOVA followed by the Tukey's test showing 95–99% significance level. The PCA was used for statistical analysis to identify unique characteristics of each irrigant tested against the biofilms from the original spectral data. Data were also analyzed using the *post-hoc* Fisher's least-significant difference analysis for multiple comparisons at $p < 0.05$.

5. Results

Table 1 shows the values of elastic modulus of different experimental dentine sections are essentially the same as the bulk tissue value. No significant differences were obtained using One-Way Anova amongst control (5.5 ± 0.9), 3.5% QIS (4.4 ± 1.1) and 6% NaOCl (2.9 ± 1.4) specimens ($p < 0.05$). Fig. 1 includes the representative data from all experimental groups at locations in each root dentine specimen. The images depict high peaks in control and 6% NaOCl+2% CHX specimens indicating presence of some biofilms. The experimental specimens treated with QIS irrigants demonstrated a great effectiveness in the action against formed biofilm with peaks upto 1.1 μm .

It is clear from the results that the surface free energy of QIS specimens was higher than compared to other specimens. Table 1 shows that the QIS irrigation protocol increased the surface free energy with highest proportion of polar component. It can be seen that surface free energies for all specimens were different with increased values in 2% QIS (107.4 ± 17.8 mJ/m²) and 3.5% QIS (146.7 ± 9.9 mJ/m²) specimens promoting spreading of the irrigant. As compared to control specimens (69.4 mJ/m² \pm 22.1), the values for 6% NaOCl+2% CHX (87.8 mJ/m² \pm 26.7) were significantly higher. This was due to differences in the polar components of different specimens. The estimated $\gamma_{\text{S}}^{\text{D}}$ values remained different for all QIS specimens as increased values not just compared to controls, but also when compared to 6% NaOCl+2% CHX specimens.

The MC3T3 cells showed ascending in the line graphs for cell viability as time lapsed. They were observed to have significantly reduced in 6% NaOCl+2% CHX treated specimens compared to the control and QIS treated specimens at 6, 12, 36 and 72 h ($p < 0.05$). However, the viability of cells in the con-

trol group (Table 1) was significantly lower at 36 and 72 h ($p < 0.05$) when compared with QIS specimens. Moreover, no significant differences were observed between the QIS specimens (0.8–0.9 OD) at any given indicated time point ($p < 0.05$).

The changes in the chemical compositions of biofilms grown by different irrigation protocols were characterised using Raman spectroscopy (Fig. 2). There were several variations in peak intensities observed after treatment of treated groups where signature spectral peaks at 730 cm⁻¹, 484 cm⁻¹, 1580 cm⁻¹ and 1670 cm⁻¹ were observed. The band at 730 cm⁻¹ is a strong band (Fig. 2A) attributed to the main components of a peptidoglycan, the C–N stretching mode of N-acetyl-D-glucosamine or N-acetylmuramic acid. The intensity decrease at 730 cm⁻¹ in 3.5% QIS specimens is due to disruption of purine bases. This can be correlated to the effect of QIS also seen in the 2% specimens. Different from QIS specimens, it was observed that DNA/purine entities were expressed in increased intensities in control, 6% NaOCl + 2% CHX and 6% NaOCl alone specimens. The bands around 480–490 cm⁻¹ exhibited changes with different irrigation protocols (Fig. 2B). The bands were assigned to the ring 'breathing' of polysaccharide chains of the polysaccharide linkages. There was a striking reduction in signals in QIS specimens as compared to the NaOCl and control specimens which showed the presence of overlapped maxima with highest intensity signal seen in control specimens ($p < 0.05$) originating from the COC ring deformations. A similar decrease was seen in QIS specimens in the intensity of the peaks at 1575 cm⁻¹ region, also referring to Amide II region and assigned to the ring-breathing modes of RNA/DNA bases, such as uracil, cytosine, adenine, guanine and thymine appearing at different positions in different specimens (Fig. 2C). The identified bands were the proteins as the main discriminant components for the biofilm formed and grown. The Amide I bands of the spectra are related to the molecular polypeptide chains of Type I collagen. The superimpositions of the Raman spectra within this region indicated increased intensities for QIS specimens with concomitant reduction in the intensity in NaOCl and control specimens (Fig. 2D). The PCA plots obtained from the biofilms (Fig. 3 A–B) formed on substrates showed that *E. faecalis* could be differentiated significantly. The loadings of the PCs show the spectral variabilities at molecular level with loadings observed at PC1 and PC2 in 837 cm⁻¹, 1662 cm⁻¹, and 1046 cm⁻¹ on dentine substrates of different groups (Fig. 3C), the highest loadings being the 6% NaOCl + 2% CHX and control specimens.

High magnification TEM images of root dentine exposed to different irrigation protocols are shown in Fig. 4. As a general pattern, all specimens showed varying degrees of structural changes. Control specimens showed no loss of surface integrity with presence of collagen network seen when sectioned perpendicular to their c-axis (Fig. 4A). Similar three-dimensional collagen network was observed in 2% QIS specimens (Fig. 4B). The specimens of 6% NaOCl + CHX showed some surface disruption and erosion of the collagen network. There was absence of any collagen fibrillar lattice as there was deterioration observed within the collagen mesh. There were wider collagen interfibrillar spaces and shorter collagen fibrils (Fig. 4C). There was a loss of periodicity showing unidentifiable amorphous interface. High magnification

Table 1 – Measurements of elastic modulus (GPa) and surface free energy (mJ/m^2). The underpinning analysis of the apoptotic MC3T3 cells induced by *E. faecalis* infections.

Groups	Elastic Modulus GPa	Surface Free Energy mJ/m^2	osteoblastic apoptosis				
			6	12	36	72	
Control	5.5 ± 0.9 A	$69.4 \text{ mJ}/\text{m}^2 \pm 22.1$ A	0.07	0.08	0.38	0.69	α
2%QIS	3.8 ± 1.8 AB	$107.4 \text{ mJ}/\text{m}^2 \pm 17.8$ B	0.08	0.09	0.61	0.83	β
3.5 %QIS	4.4 ± 1.1 A	$146.7 \text{ mJ}/\text{m}^2 \pm 9.9$ C	0.09	0.09	0.58	0.71	∞
6%NaOCl + CHX	2.1 ± 3.1 BC	$87.8 \text{ mJ}/\text{m}^2 \pm 26.7$ D	0.05	0.06	0.09	0.23	ϕ
6%NaOCl	2.9 ± 1.4 B	$57.6 \text{ mJ}/\text{m}^2 \pm 11.8$ E	0.03	0.03	0.05	0.11	Ω

Values are means \pm standard deviation and tested by One Way Anova vertically.

Groups identified by different letters and numerals were significantly different at $p < 0.05$.

The bold values represent significant values.

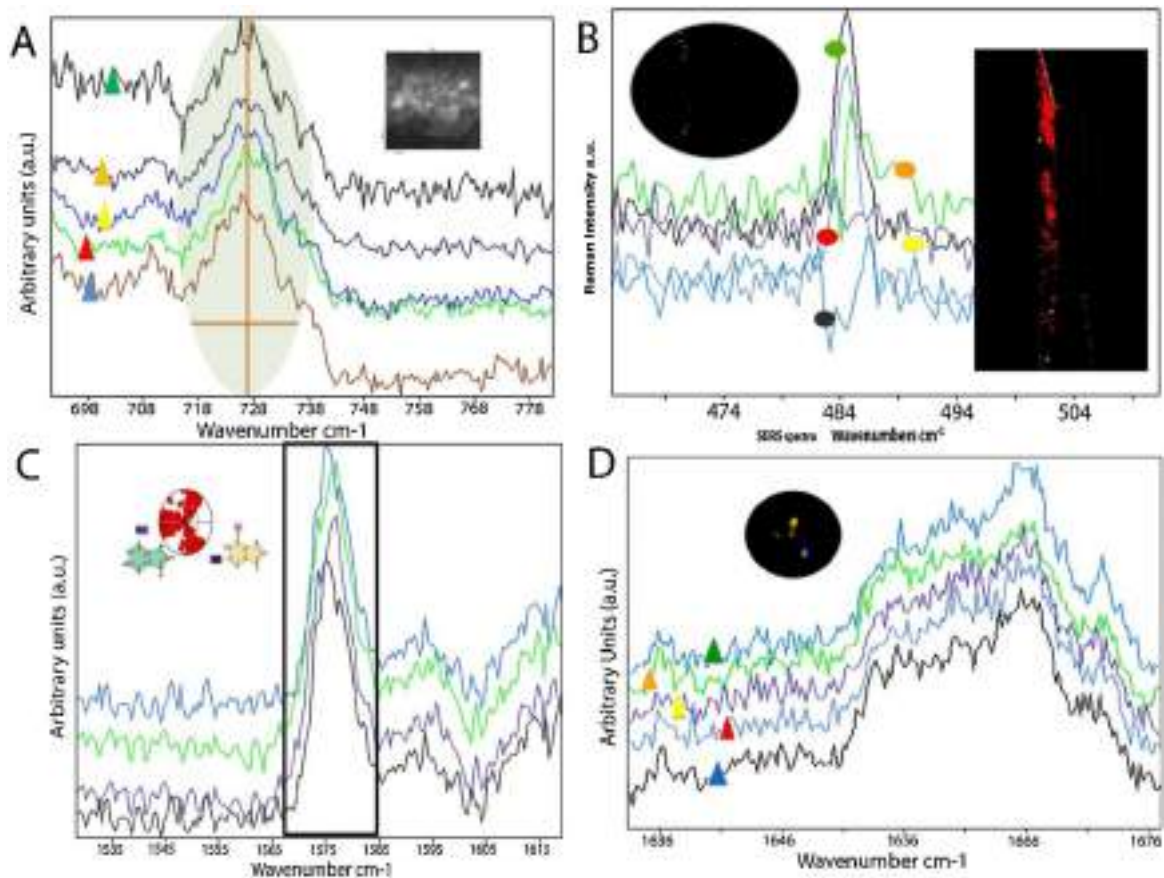


Fig. 2 – Raman spectra of *E. faecalis* biofilms on root dentine disc specimens treated with different irrigant protocols. (A) Obvious and inter-related variations at regions around Raman shifts around 730 cm^{-1} , which is assigned to bacterium; green triangle control, orange 6%NaOCl+2%CHX, yellow triangle 6% NaOCl, red triangle 2% QIS, blue triangle 3.5% QIS; **(B)** Raman spectra of biofilm matrix samples. Functional groups from biomolecules were identified where significant spectral differences of control and treated specimens can be seen in the $480 \text{ cm}^{-1} - 490 \text{ cm}^{-1}$ region after normalization. The Raman shift at this region was the region where amylopectin exopolysaccharide was detected. The Raman intensity on the y-axis represented the amount of amylopectin exopolysaccharide detected in an arbitrary unit. The spectra fall on the green, red, orange, yellow, and black regions belonging to the Raman intensity created by dentin disc specimens in control, 6%NaOCl + CHX, 6% NaOCl, 2% QIS, 3.5%QIS, groups respectively. **(C)** The peaks observed around the 1575 cm^{-1} and 1580 cm^{-1} region are assigned to the ring-breathing modes of DNA/RNA bases, the difference amongst the group is owing to the difference in irrigation protocols causing difference in damage or disruption of nucleic acids – black 3.5% QIS < dark blue < 2.5%QIS < green < 6%NaOCl+2% CHX < light blue 6% NaOCl > black saline. **(D)** The bands in the $1640-1680 \text{ cm}^{-1}$ region can be assigned to the Amide I stretching vibration of C=O; green triangle 3.5% QIS > orange 2% QIS > yellow 6% NaOCl > red 6% NaOCl + 2% CHX > black saline control.

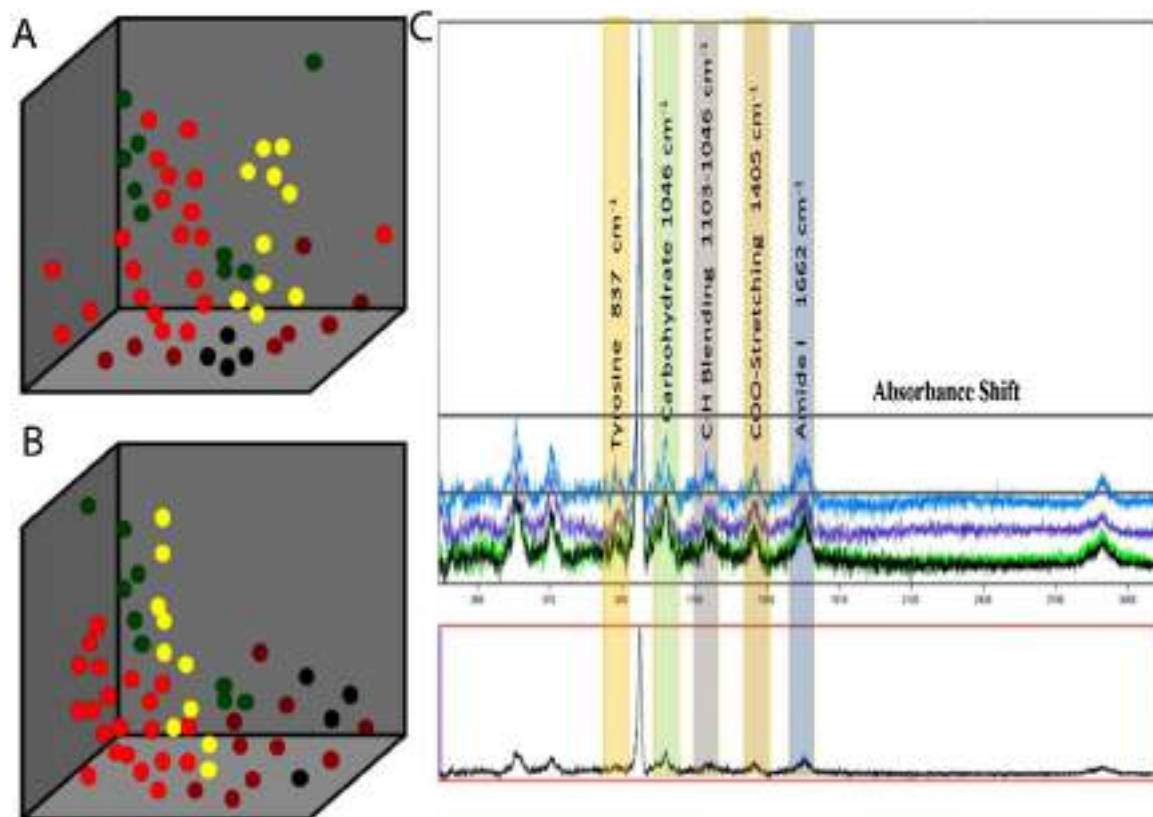


Fig. 3 – (A–B) PCA plot and components of different irrigants (black 3.5% QIS; green saline; red 6% NaOCl + 2% CHX; brown 2% QIS; yellow 6% NaOCl) used on *E. faecalis* biofilm. (C) Different bands of presented showing tyrosine, carbohydrate, C–H bending, COO stretching and Amide I shifts in different groups (blue – 3.5%QIS, purple – 2%QIS, green – Sterile Saline, black NaOCl + CHX).

6% NaOCl alone irrigated root dentine specimens showed no specific cross banding (hand arrow), although individual collagen fibres were observed at 10 nm level. Moreover, the collagen fibrils periodicity and gap/overlap zones were clearly invisible in 6% NaOCl + 2% CHX when seen in high magnification TEM images (Fig. 4C). The 3% QIS specimens showed an intact dense collagen fibrillar network with well-formed collagen. There was integrity in the protein structure and showed uniformity as compared to other specimens (Fig. 4E). High magnification images of the same specimen showed periodicity of the collagen fibrils with visible D-banding reflecting the precision of $\alpha 1$ and $\alpha 2$ preserved alignment (Fig. 4F).

Representative CLSM images of single-species *E. faecalis* biofilms grown on root dentine discs following treatment with different irrigating solutions are shown in Fig. 5 respectively. Viable cells were stained green and dead cells were stained red. The *E. faecalis* control specimens showed densely clustered extensive green colonies (94.33 ± 2.1 , $p = 0.1$) with minimal or no areas of dead bacterial cells (Fig. 5A–B). A top-down view of the image stack after treatment with 2% QIS irrigation protocol with marked differences in the degree of microbial coverage with biofilms consist predominantly of dead cells (71.7 ± 5.5) as revealed by the red channel in 3 and 10 day biofilms (Fig. 5C–D). Treatment with QIS irrigation protocols led to a significant increase in red areas of *E. faecalis* biofilms with the particular concentration of 3.5% QIS able to

effectively kill the majority of cells (86.7 ± 4.3) in the biofilm (Fig. 5E–F). The amount of live bacteria decreased significantly in QIS specimens, with the whole layers in 6% NaOCl + 2% CHX treated specimens almost fully appeared red (66.4 ± 6.6), with small green areas were also found (Fig. 6G–H). The live bacterial cell number was notably increased in control and 6% NaOCl + 2% CHX specimens as a reemergence in contrast to the QIS specimens, a fact that is coincident that there is incapability to form biofilm after secondary adhesion with QIS protocols, also seen in 6% NaOCl (Fig. 5I–J) specimens alone (Table 2). An overall mean of 3.6 ± 0.44 and 2.64 ± 0.11 log CFU count (CFU/mL) was registered (Table 2) for 2%- and 3.5%QIS respectively ($p < 0.05$). The mean values for CFU/mL were lowest for 3.5%QIS specimens as compared to other groups. The significantly high count was obvious in control groups (7.02 ± 0.36) which were more prone to multiplication of microbial colonies. The 6%NaOCl single groups (3.0 ± 0.99) were statistically ($p < 0.05$) similar to the 2%QIS (3.6 ± 0.44) groups in the count range.

Scanning electron microscopy images of 3.5% QIS irrigant (Fig. 6A–B) after ultrasonic irrigation protocols are seen with physical appearance of quaternary ammonium silane having formed a thin crust-type surface layer. High resolution representative SEM images of mouse fibroblast cell attached onto the root dentine surface after saline treatment (Fig. 6C). The cytoplasmic extensions or filopodium-like processes are

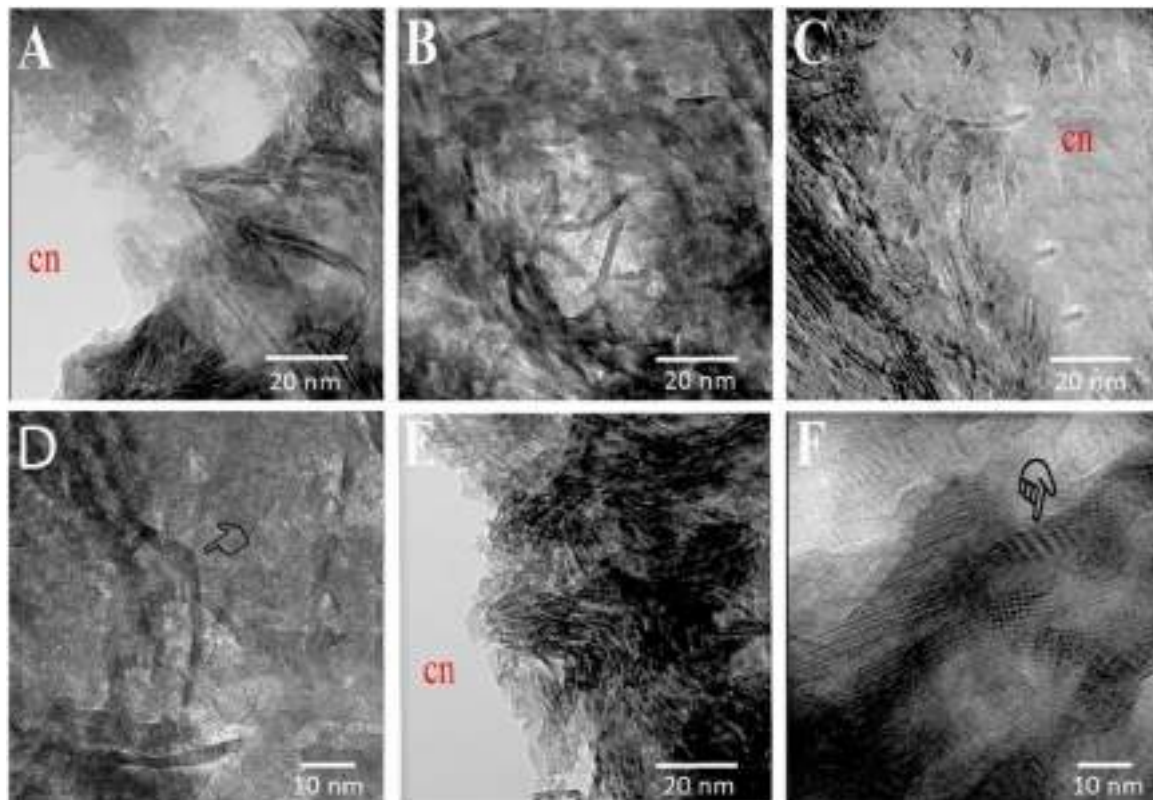


Fig. 4 – High magnification TEM images of epoxy resin-embedded root dentine after following experimental irrigation protocols. (A) Sterile saline irrigation; (B) 2% QIS irrigant treatment; (C) 6%NaOCl + CHX irrigation showing collagen degradation with no uniformity in periodicity pattern, unravelling and loss of banding; (D) High magnification 6% NaOCl alone irrigated root dentine showing no specific cross banding (arrow), although individual collagen fibers were observed at 10 nm level; (E) 3.5% QIS irrigation protocol showing presence of organized collagen fibrillar lattice with preservation of well-formed collagen fibril structure and presence of (F) scission of the microfibrils into short, individual fragments showing dominant cross banding and well preserved structures – cn > canal.

Table 2 – Bacterial viability and CFU log in *E. faecalis* biofilms following different irrigant treatments on dentine.

	Dead	Live	log CFU/mL	post-hoc Fisher's least-significant difference analysis for multiple comparisons at $p < 0.05$						
	Mean \pm SD									
<i>E. faecalis</i>										
Control	5.67 \pm 7.1	94.33 \pm	7.02 \pm	$p = 0.07$	$p = 0.87$	$p = 0.03$	$p = 0.1$	$p = 0.11$	$p = 0.09$	
	A	2.1 β a	0.36a							
2%QIS	71.7 \pm 5.5	22.3 \pm 5.4	3.6 \pm	$p = 0.04$	$p = 0.06$	$p = 0.03$	$p = 0.00$	$p = 0.01$	$p = 0.05$	
	B	λ b	0.44b							
3.5 %QIS	86.7 \pm 4.3	13.3 \pm 3.3	2.64 \pm	$p = 0.01$	$p = 0.00$	$p = 0.00$	$p = 0.00$	$p = 0.00$	$p = 0.00$	
	C	∞ c	0.11c							
6%NaOCl + CHX	66.4 \pm 6.6	33.6 \pm 7.1	4.12 \pm	$p = 0.06$	$p = 0.09$	$p = 0.1$	$p = 0.2$	$p = 0.4$	$p = 0.00$	
	D	θ d	0.28d							
6%NaOCl	70.3 \pm 3.3	29.7 \pm	3.0 \pm	$p = 0.08$	$p = 0.07$	$p = 0.4$	$p = 0.3$	$p = 0.1$	$p = 0.00$	
	D	6.6]e	0.99b							

CHX: chlorhexidine, QAS: quaternary irrigant solution; NaOCl: sodium hypochlorite.

Values are means \pm standard deviation and tested by One Way Anova vertically. ($n = 3$).

Groups identified by different numerals and letters were significantly different vertically amongst groups at $p < 0.05$.

Small alphabets identify different groups amongst live and dead cells.

Concentration of QIS molecule and NaOCl + CHX based on Fisher's protected least significant difference.

thickly spread over and integrating closely to the root dentine disc. In contrast, the 6% NaOCl + CHX treated cells (Fig. 6D) showed different morphologies with shrinkage and limited

projections of cytoplasm with open blebs formed on the cell cytoplasm covering the dentine substrate. Moreover, a small number of rounded-shaped cells in the representative images

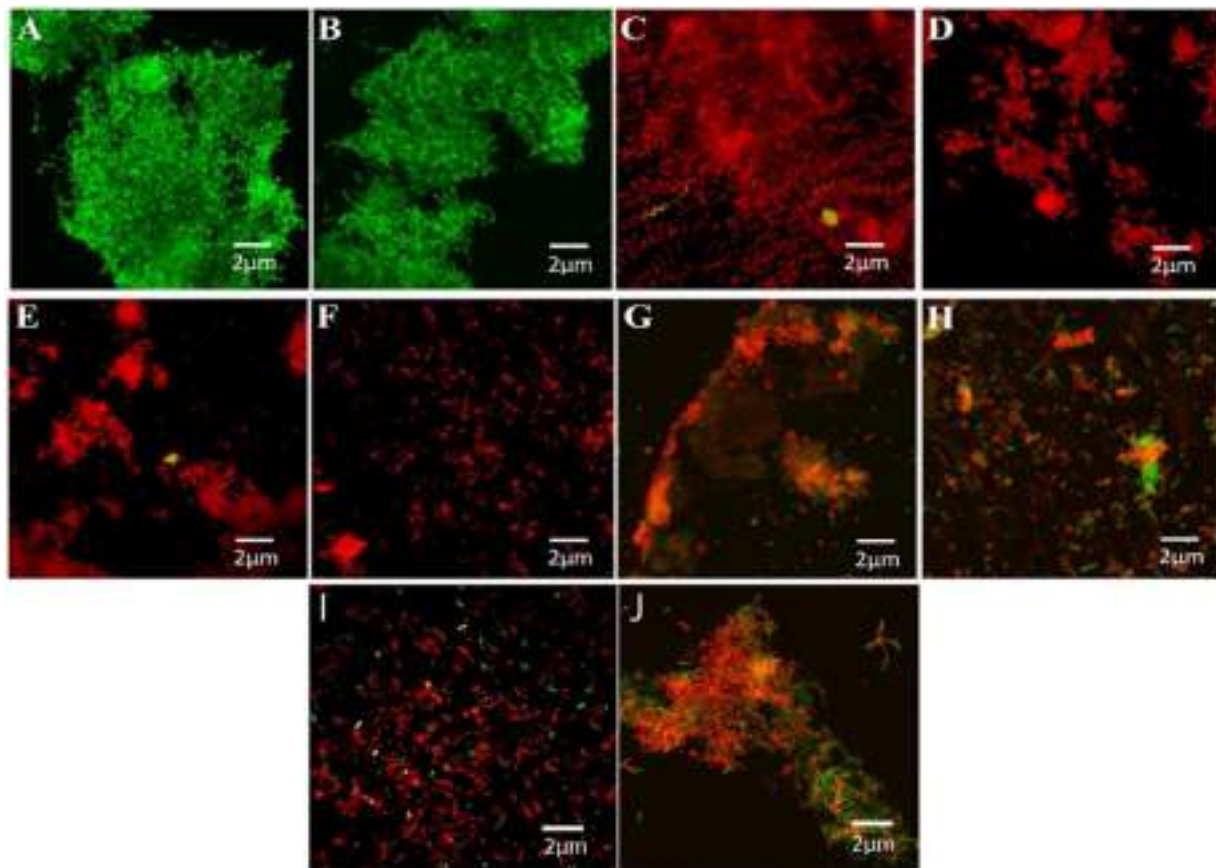


Fig. 5 – CLSM images of *E. faecalis* biofilms subjected to growth and irrigation protocols after 3 and 10 days using Live/Dead[®] viability stain with the green color indicating live cells and the red color showing the dead bacteria. (A-B) Tilt view (~30°) illustrating green emission in control specimens after 10 days. (C-D) Top-down view of the image stack after treatment with 2% QIS irrigation protocol with marked differences in the degree of microbial coverage with biofilms consist predominantly of dead cells as revealed by the red channel in 3 and -10 day biofilms; (E-F) CLSM merged image after application of new 3.5% QIS irrigant after 3 and -10 days respectively; (G-H) specimens showing 20 µm stack of 6% NaOCl+2% CHX ultrasonic specimens showing some emergence of biofilm growth after 10 days; (I-J) 6% NaOCl treated specimens.

were observed. Cells with large cytoplasm and projections similar to the saline group were observed in 2% QIS and 3.5% QIS specimens respectively (Fig. 6E-F). These specimens showed increased cell viability and proliferation compared to other samples. The cellular morphology did not appear perturbed with cells exhibiting normal fibroblasts morphology with increased number of cells spread onto the root dentine surface. NaOCl alone treated specimens showed fibroblasts exhibiting an altered morphology with round shape (Fig. 6G) and small size and presence of ill-defined cytoplasmic membrane suggestive of cell necrosis. Three-day *E. faecalis* biofilm (Fig. 6H) showed an increase in the number and density of the bacterial microcolonies that are almost covering the entire dentinal surface after saline treatment. The bacteria were completely eradicated of bacterial colonies after the use of 3.5% QAS protocols (Fig. 6I). Moreover, QIS 3.5% (data not shown) showed phase separation in the presence of water present inside dentinal tubules after ultrasonication. The formation of sealer tags in 3.5% QIS irrigated specimens are seen in representative SEM images of sealer-dentine interphase penetrating deep into the dentinal tubuli appearing as smooth tubular rods.

A typical Axiovert microscope (Carl Zeiss) image of stained with MitoTracker green is shown in Fig. 7. The experiments confirmed that MitoTracker accumulates in mitochondria and also shows fluorescence enhancement when accumulated inside the organelles. The cells were devoid of staining or had fragmented staining in 6% NaOCl + 2% CHX and 6% NaOCl treated cells (Fig. 7B&E) as compared to control specimens (Fig. 7A) where individual mitochondria were stained. Cells treated with 6% NaOCl + 2% CHX demonstrated a dramatic loss of Mitotracker staining. Fig. 7D depicts a low power reconstruction with significantly stained mitochondria in cells treated with 3.5% QIS. A few stained cells were also found in 2% QIS specimens (Fig. 7C).

6. Discussion

The research questions mentioned regarding quaternary ammonium silane irrigant solution will be justified for its significant potential for future commercialization for endodontic applications. Adequate shaping and cleaning procedures of the root canal system are amongst the clinical challenges

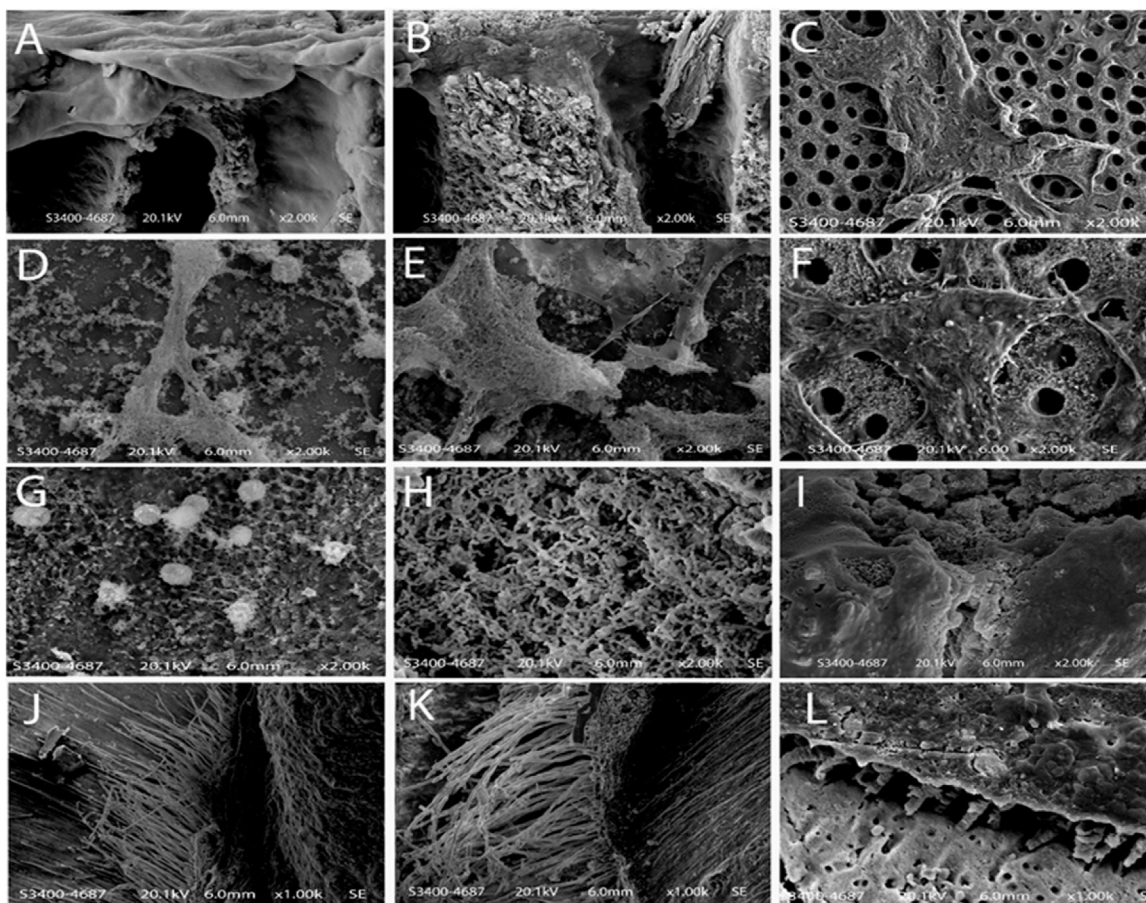


Fig. 6 – Representative SEM images of root dentine following application of (A–B) 3.5% QIS irrigant after ultrasonic irrigation protocols. The physical appearance of quaternary ammonium silane was seen to form a thin crust. (C) High resolution representative SEM of mouse fibroblast cell attached into the root dentine surface after saline treatment. The cytoplasmic extensions or filipodium-like processes are thickly spread and bound closely to the root dentine disc. In contrast, (D) the 6%NaOCl + CHX treated cells showed different morphologies with limited projections of cytoplasm and open blebs formed on the cell cytoplasm covering the dentine substrate and a small number of rounded-shaped cells in the representative images. (E–F) Cells with large cytoplasm and projections similar to the saline group were observed respectively in 2%QIS and 3.5%QIS specimens respectively. The cellular morphology did not appear disturbed with cells exhibiting normal fibroblasts morphology with increased number of cells spread onto the root dentine surface. (G) 6% NaOCl treated specimens showing fibroblasts exhibiting an altered morphology with round shape and small size with presence of ill-defined cytoplasmic membrane suggestive of cell necrosis. (H) 3-day *E. faecalis* biofilm showing an increase in the number and density of the bacterial microcolonies that is almost covering the entire dentinal surface after saline treatment; (I) complete eradication of bacterial colonies seen after using 3.5% QAS protocols; (J–K) formation of sealer tags in control and 3.5%QIS irrigated specimens in representative SEM image of sealer-dentine interface; (L) 6%NaOCl + 2% CHX specimen.

during root canal treatment procedures [39]. The success and longevity of root canal treatment is culminated in a predictable outcome with the adequate action of irrigant protocols as the major reasons for failure, usually cited due to recurrence of infection [40]. No irrigant solutions available meet all the requirements set for an ideal irrigant [41] covering antibacterial spectrum, dissolution of remnants of necrotic and vital pulp tissue and removal of smear layer during the root preparation [40]. The normal practice has been the use of irrigant solution combinations with alternate chelators to overcoming some shortcomings [42]. Irrigant solutions used have unique distinctive properties, such as NaOCl which has a broad antibacterial spectrum [43] but is a potential irritant

to periapical tissues [39]. Conversely, CHX is less cytotoxic to the periapical tissues as compared to NaOCl, but does not dissolve the pulp tissue [44]. The use of NaOCl and CHX (as an adjunct) in root canal irrigation is to improve antimicrobial properties. However, the issue at hand is still controversial, and remains unclear in literature, as which natural root properties could be affected by different irrigant solutions [45]. Prolonged acidification due to aciduric microbiota changes the ecological balance within the tooth substrate increasing the bacterial influence [46]. Untreated necrotic root canals are dominated by proteolytic anaerobic organisms, whereas a diverse community dominate the treated root canal system [47]. *E. faecalis* colonies are known to survive in harsh

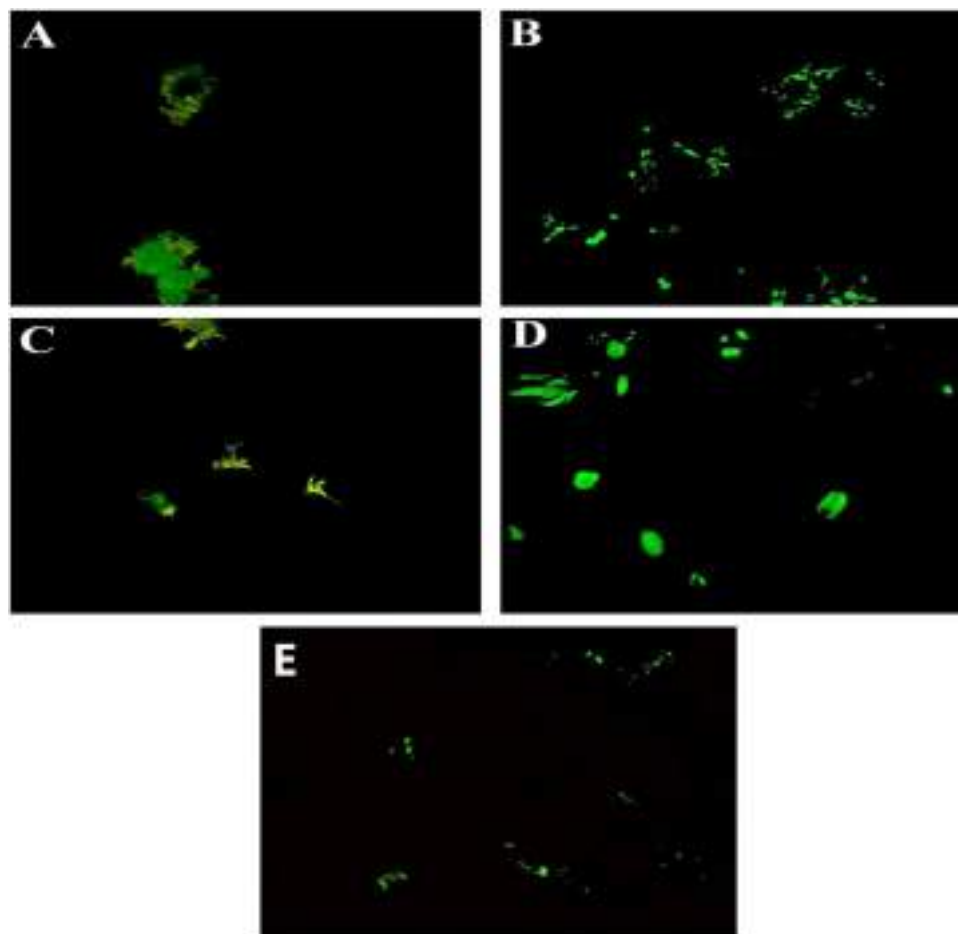


Fig. 7 – (A-D) 3T3 NIH Mouse fibroblastic cells incubated with 200 nM MitoTracker Green (mitochondria-specific fluorescent dye) for 15 min, and analysed with an Axiovert microscope (Carl Zeiss) equipped with a Neofluar 100 NA 1.3 objective. (A) Sterile saline, (B) 6%NaOCl+2%CHX, (C) 2%QIS and (D) 3.5 %QIS and (E) 6%NaOCl treated cells showing different levels of mitochondria disintegration.

condition with reinfections prevailing upto 24%–77% [48]. For that purpose, NaOCl combined with chelating agents have been used to remove the smear layer and biofilms during root canal instrumentation [49]. NaOCl has been known to form precipitates and surface discoloration [24] when combined with CHX providing inadequate sealing of the obturating material [50]. That being said, an intermediate irrigating solution such as saline or distilled water followed by drying of the root canals is suggested. The experimental specimens treated with QIS irrigants demonstrated a great effectiveness in the action against formed biofilm with peaks up to 1.1 μm .

The multipotent antimicrobial action of QAS/K21 has gained attention [25,26], especially for disrupting bacterial membranes leading to leakage of intracellular cytoplasm and cell death [unpublished data]. In the current study, a new in vitro model was developed that was reproducible and allowed the simulation of an in vitro closed system. All irrigant solutions were subjected to challenging environmental conditions with aggressive exposure to growing biofilms in both phases of initial growth and after the endodontic treatment. The effect of irrigant delivery and activation methods

to enable a carry-over antimicrobial effect was kept in consideration. The sterile saline had no effect on the microbial killing, mechanical, mitochondrial or Raman spectral change, compared to other experimental groups with no difference in biofilm viability. Therefore, use of chemically active disinfectant is pivotal for microbial killing, and not just an agitation method [51]. In order to verify a new endodontic irrigant, a modified quaternary ammonium silane was selected to analyse its mechanical and biological impact on the root dentine.

There is increased surface free energy in 3.5% QIS ($146.7 \pm 9.9 \text{ mJ/m}^2$) specimens which might be due to probable surface roughness as a result of QAS surface crust. One explanation might be the polar and non-polar components of the irrigants dispensed onto the root canal components. Using samples of silica sol-gel solutions, a significant increase ($p < 0.05$) in the contact angle could be observed showing also increased hydrophobic properties, especially increasing hydrophobicity. The increased water repellence as a function of saline present inside the root canal could also be explained for the increase in roughness [52], which can also be attributed to the ethanol content. The droplet volume and substrate type were equal after calculations, as it looks apparent that the irriga-

tion contents may have caused the difference in discrepancies (Table 1). There are changes in the γ_{S^h} values which may also reflect an increase in the surface density on the root dentine surface [53].

The underpinning mechanism responsible for osteoblastic apoptosis via *E. faecalis* infection indicates a viable impact (Fig. 2). An antimicrobial strategy using QIS irrigant was developed and proved to effectively eliminate *E. faecalis* without a cytotoxic effect on the osteoblastic cell line. Inflammatory destruction of bone is persistently found in apical periodontitis resulting in a detrimental effect on bone remodelling [54]. A strong relationship occurs between osteoblastic apoptosis and infecting microorganisms found in oral bone diseases as bacterial infection can promote the process as one of the central hubs of disease formation [55]. In the current study, the proliferation of the infected cells was found to be suppressed for 72 h after using 6% NaOCl + 2% CHX and 6% NaOCl. These results may suggest the biological influence between the viable and non-viable *E. faecalis* in relation to osteoblastic viability. Measurements of the expression of cells after treatment with QIS specimens show increased numbers of murine osteoblasts which should be associated with the virulence factors of the bacteria. Nevertheless, this may be influenced by the QIS irrigant. These findings might provide deeper insight into the development and repair of periapical bone destruction. Further investigations are needed to explore the relevance of *E. faecalis* infections and the strains selected against the osteoblastic cells as the underlying mechanisms still remain to be elucidated.

The Raman shift where the peak intensities were recorded and converted into mean value with standard deviation are shown in Fig. 2. The characteristic band at 730–733 cm^{-1} showed a complete shift and change in intensity based on the irrigant used. This band can be attributed to only one vibrational mode, which actually are only those vibrational containing nitrogen [56]. Moreover, the C–N stretching vibration is also not attributed to this complex spectral feature. Instead it is assigned to the in-plane pyrimidine and imidazole ring 'breathing' mode [57], a broadening of this specific peak was seen for the biofilms. The intensity changes in the peaks demonstrate a decrease of protein, pyocyanin and carbohydrate contents in specimens treated with QIS, deriving from purine bases [58]. The intensive signals at 484 cm^{-1} were assigned (Fig. 3B) to the polysaccharides [59] detected in all samples. Based on the comparability of different spectra, 3.5% QIS specimens showed the least amount of intensity followed by 2% QIS > 6% NaOCl + 2% CHX specimens. These spectroscopic finger prints of carbohydrates appeared dull and broad being affected with higher concentrations of QIS. In addition, the Raman bands around 1666–1667 cm^{-1} are designated to the lyophilized lectins in the Amide I region, where as 1575 cm^{-1} bands were assigned to the ring-breathing modes of DNA/RNA bases, such as adenine, cytosine, guanine, thymine, and uracil appearing at different positions in different specimens [60]. These amyloids stabilize the biofilm matrices describing the β -sheet proteins of the Amide I regions. These bands were strongly observed in the EPS bands of control specimens, but having lower intensities in the QIS specimens. The accompanying spectroscopic Raman analysis, CLSM images and decrease in CFU log count was

evident and in line with the rejection of the null hypothesis that there is no difference in antibacterial properties of QIS used as a potential endodontic irrigant when compared to other potent solutions (NaOCl, NaOCl + CHX). This could overcome any short comings of existing endodontic irrigants.

The quaternary ammonium silane has strong antibacterial properties as it does not enter into the cell due to the interference of ion transport mechanism [61]. N^+ of the positively charged quaternary group within the pyridinium ring causes a breakage of cell membrane due to its high affinity towards it. This is resulting in massive discrepancy and collapse of the cell because of its own osmotic pressure. This is aided by the long-chain lipophilic alkyl chains, making the action appear strong, long, and rapid [62]. Spectroscopic techniques have been successfully used for long for identification of bacterial components within the biofilm structure at molecular level hypothesizing that more bacterial colonies are being affected at higher concentrations of QAS. Furthermore, the QIS crust formation remains active and available for contact killing for seven days and does not allow regrowth of bacteria. This difference is consequential to the released amount of QIS within the bacterial suspensions or biofilms present within the root specimens. The sol-gel based QIS solution provides a facile method for the synthesis of organosilicates with the tetrafunctional based organosilane anchoring unit forming a three-dimensional network to be formed once condensation is brought to completion within the dentinal substrate. This inadvertently minimizes the possibility of QIS molecules to leach out of the dentine surface providing longer antimicrobial activity. This layering of the QIS solution had contributed well in terms of better dispersion, substantivity and infiltration on the dentin surface.

Dentine collagen matrix contributes to the fatigue resistance and viscoelasticity [63]. The presence of apatite crystals protect the collagen fibrils from degradation [64]. However, based on the TEM observations, chemical degradation of fibrils was seen in specimens irrigated with NaOCl as the organic phase of root dentine is deproteinized via a diffusion control mechanism. The authors speculate that the disappearance of D-spacing in individual collagen fibers in specimens treated with 6% NaOCl could also disappear due to non-assembly of collagen fibers as characteristic D-period is established due to lateral assembly of correctly aligned microfibrils [65]. The authors conclude that the collagen sparse zone contained irregular deproteinized sections facilitating penetration of 6% NaOCl + 2% CHX with absence of cross-banding seen within individual collagen fibers on higher magnification. This is primarily due to the OCl^- ion, a chlorine reflective [66] associated with increased proteolytic activity and thereby destruction of the collagen matrix [67]. The absence of cross-banding in the specimens is unknown, indicating weakened fibrils owing to the lack of cross-links within the triple helices, probably being bacterial ingress, more compared to QIS specimens destroying the hydrogen bonds which are essential for holding the triple helix together. Given this, QAS/K21 is a known inhibitor of MMPs and cysteine cathepsins increasing the resistance of dentine collagen against degradation [27]. The collagen fibres appeared unaffected in QIS specimens and cross-banding was visible. Now, k21 is known not to promote formation of apatite

crystals, but the silicon (-Si-C-) present within the silane formulation can act as nucleation site [68]. Within the root canal system, the apatite crystallites in the QIS specimens may help in blocking the dentinal tubuli preventing the bacterial invasion [69]. The QAS are known to bring stabilisation as a result of formation of molecular siloxane bridges despite the temporal hydrolytic stability rejecting the null hypothesis that the irrigant has no effect on mechanical properties seen in the current AFM experiments (Table 1). On-going work is being performed to study mechanical properties in depth after QIS use.

The root dentine surface after irrigation protocols and effect of biofilm on the substrate was examined using SEM. There were thick deposits of QIS with detrimental full coverage of dentinal tubuli visible in specimens. The purpose of the present research was not to study the deposition and nature of deposits on the root dentine surface, including the deposits formed as a result of NaOCl and CHX combination. It is worth noting, that NaOCl/CHX combination has a potent antimicrobial activity [70,71], and hence an addition as a group was added in this study. However, clinicians should be aware of potential interactions and hazards of using this combination in clinical practice, and all recommended guidelines should be followed to prevent/minimize the formation of the brown precipitate in the root canal space. The 3.5% QIS irrigant did not seem to exert any cytotoxic effects on the NIH 3T3 cells (2% QIS data not shown). There was no alteration in cell morphology with mouse fibroblast cells attached to the root dentine surface with cytoplasmic extensions or filipodium-like processes thickly spread and bound closely to the root dentine disc. This was similar to the control specimens and results previously published with cross-linked quaternary ammonium polymers [72]. By contrast, 6% NaOCl + 2% CHX groups showed alteration in cell morphology with limited projections of cytoplasm and open blebs formed on the cell cytoplasm covering the dentine substrate and a small number of rounded-shaped cells in the representative images. Further, this combination added no value in the field of endodontics, rather compromises the debridement of the root canal system and three dimensional seal in obturation. This change in cell morphology was seen more drastic in specimens treated with 6% NaOCl. The fact that QIS irrigants were compatible and lethal to bacteria was expected. There is a strong possibility that the proteins and other nutrients from the cell medium could have attached and covered onto the cells, reducing the effect of the irrigant. This could partially explain these results obtained. It is noteworthy that NaOCl is a known to induce genetic damage [73] representing a potential alert for its potency and use in endodontic practice. Moreover, the quaternary ammonium silanes are water scavengers hydrolysing alkoxy groups and reacting with water molecules, finally converting the attached silanes to silanol molecules [74]. This will lead to phase separation in the presence of water from dentinal tubuli which are producing spherical structures after ultrasonication. The length of resin tags appeared adequate in 3.5% QIS groups despite the crusts type deposition on the root dentine. The resinous affinity of organosiloxane groups of QAS may have directly resulted in better penetration of resin sealer, compared to 6% NaOCl + 2% CHX specimens (data not shown). The experiments con-

ducted confirmed accumulation of MitoTracker green inside the mitochondria. The fluorescent enhancement was seen at different levels of mitochondria disintegration. In the current study, the effects of QAS and exposure were evaluated as QAS did not show mitochondrial defragmentation. Fluorescence microscopy revealed mitochondrial defragmentation in NaOCl specimens. Although the physiological significance of the dynamics of mitochondrial morphology is not completely understood, a detailed comparison of the antimicrobial efficacy and mitochondrial inhibitory effects of the QIS needs to be performed to identify high antimicrobial efficacy and with minimum mitochondrial effects.

The null hypothesis was rejected as there was a difference in bactericidal effect against *E. faecalis* biofilms. Bacterial biofilms are complex three dimensional structures in which bacteria are embedded mainly due to the actions of exopolysaccharides. The activation of a biochemical stress response and changes in the cell membrane makes the biofilms more sensitive to the antimicrobial agents. All endodontic infections are biofilm induced as bacteria survive in an adaptive mechanism persisting the endodontic infection [75]. The irrigation protocol of 3.5% QIS showed great potential of to render antibacterial properties without a discernible decrease. This contact killing in presence of TEOS, are covalently bonded showing completely dead cells (86.7 ± 4.3) due to the silanol groups covalently bonded via $-O=Si-O-$ linkages circumventing or slowing down the growth of biofilms even in the secondary adhesion phase. The current result was further validated by an intensive Raman study. The NaOCl specimens significantly reduced the biofilm but cannot render the canals bacteria free.

The present study evaluated the effects of QIS irrigant solution on the attachment, differentiation of NIH 3T3 fibroblast cells, *E. faecalis* biofilms and root dentine. Previous studies have shown the cytotoxicity effects of NaOCl and CHX which was dose dependant [76,77] showing stem cell inhibition [78]. Considering this issue, the authors evaluated alexidine and its antimicrobial effect. In addition to QIS, alexidine alters cell permeability with a higher virulence for bacteria [79]. No precipitate was observed from the alexidine and QAS combination. EDA, a significant part of the mix, is known to improve surface wettability promoting cell attachment via increased attachment of fibronectin [80]. Because of elevated alkalinity, the presence of NaOH circumvented the dissolution of organic matter through saponification of fats [81]. The NaOH present within the formulation provides ions to EDTA turning the disodium into trisodium > pentasodium [82]. The authors found that the ability to dissolve organic tissue in an alternating irrigating regimen is not efficient because of absence of NaOCl. This finding has prompted us to indicate the use of EDTA with QIS as a final and only rinse, and irrigant. More predictable reduction of intracanal bacteria is ascribed to the use of this new strategy providing a favourable endodontic profile enhancing the versatility of the material and its potential use in endodontics. Future work is underway in the development of the irrigant formulation to investigate the detailed effects of QIS on undifferentiated stem cells and bacterial lipopolysaccharide membranes looking at its important role in regenerative endodontics.

7. Conclusion

The novel QIS root canal irrigant achieved optimum antimicrobial protection inside the root canals compared to 6% NaOCl alone, 6% NaOCl + 2% CHX. In fact, the use of the novel 3.5% QIS irrigant facilitated a toxic effect against the *Enterococcus faecalis* biofilm. In a complex endodontic system there is a potential to exploit the QIS irrigant for a feasible therapeutic approach against biofilm infection.

Significance

In a complex root canal system, there is a potential to exploit QIS irrigant for a feasible therapeutic approach against biofilm infection offering a sufficiently large therapeutic window.

Funding

The work was supported by IMU JC Grant number (IMU 425/2018) and KHG fiteBac Technology.

Acknowledgements

The authors thank the labs at IMU, Mimos Research Center, University of Malaya and University of Western Australia for the research experiments and analysis. The k21/QIS irrigant raw materials used in this study was supplied by KHG fiteBac Technology, Marietta, GA, USA and modified by Dr Umer Daood at IMU lab.

REFERENCES

- [1] Gomes BP, Pinheiro ET, Gade-Neto CR, Sousa EL, Ferraz CC, Zaia AA, et al. Microbiological examination of infected dental root canals. *Oral Microbiol Immunol* 2004;19:71e76.
- [2] Ricucci D, Siqueira Jr JF. Biofilms and apical periodontitis: study of prevalence and association with clinical and histopathologic findings. *J Endod* 2010;36:1277–88.
- [3] Nair PN, Henry S, Cano V, Vera J. Microbial status of apical root canal system of human mandibular first molars with primary apical periodontitis after a “one-visit” endodontic treatment. *Oral Surg Oral Med Oral Pathol Oral Radiol Endod* 2005;99:231–52.
- [4] Siqueira Jr JF, Rôças IN. The microbiota of acute apical abscesses. *J Dent Res* 2009;88:61–5.
- [5] Sakamoto M, Rôças IN, Siqueira Jr JF, Benno Y. Molecular analysis of bacteria in asymptomatic and symptomatic endodontic infections. *Oral Microbiol Immunol* 2006;21:112–22.
- [6] Gomes BPFA, Pinheiro ET, Gadê-Neto CR, Sousa ELR, Ferraz CCR, Zaia AA, et al. Microbiological examination of infected dental root canals. *Oral Microbiol Immunol* 2004;19:71–6.
- [7] Zhang C, Du J, Peng Z. Correlation between *Enterococcus faecalis* and persistent intraradicular infection compared with primary intraradicular infection: a systematic review. *J Endo* 2015;41:1207–13.
- [8] Saleh IM, Ruyter IE, Haapasalo M, Ørstavik D. Survival of *Enterococcus faecalis* in infected dentinal tubules after root canal filling with different root canal sealers in vitro. *Inter Endo J* 2010;37:193–8.
- [9] Ghorbanzadeh A, Fekrazad R, Bahador A, Ayar R, Tabatabai S, Asefi S. Evaluation of the antibacterial efficacy of various root canal disinfection methods against *Enterococcus faecalis* biofilm. An ex-vivo study. *Photodiag Photodyn Ther* 2018;24:44–51.
- [10] Vera J, Siqueira Jr JF, Ricucci D, Loghin S, Fernandez N, Flores B, et al. One- versus two-visit endodontic treatment of teeth with apical periodontitis: a histobacteriologic study. *J Endod* 2012;38:1040–52.
- [11] Marinho AC, Martinho FC, Zaia AA, Ferraz CC, Gomes BP. Monitoring the effectiveness of root canal procedures on endotoxin levels found in teeth with chronic apical periodontitis. *J Appl Oral Sci* 2014;22:490–5.
- [12] Crane AB. A predictable root canal technique. Philadelphia: Lea & Febiger; 1920.
- [13] Du T, Wang Z, Shen Y, Ma J, Cao Y, Haapasalo M. Effect of long-term exposure to endodontic disinfecting solutions on young and old *Enterococcus faecalis* biofilms in dentin canals. *J Endod* 2014;40:509–14.
- [14] Hand RE, Smith ML, Harrison JM. Analysis of the effect of dilution on the necrotic tissue dissolution property of sodium hypochlorite. *J Endod* 1978;4:60–4.
- [15] Cullen JK, Wealleans JA, Kirkpatrick TC, Yaccino JM. The effect of 8.25% sodium hypochlorite on dental pulp dissolution and dentin flexural strength and modulus. *J Endod* 2015;41:920–4.
- [16] von Arx T, Bosshardt D. Vertical root fractures of endodontically treated posterior teeth: a histologic analysis with clinical and radiographic correlates. *Swiss Dent J* 2017;127:14–23.
- [17] Sim TP, Knowles JC, Ng YL, Shelton J, Gulabivala K. Effect of sodium hypochlorite on mechanical properties of dentine and tooth surface strain. *Int Endod J* 2001;34:120–32.
- [18] Garcia AJ, Kuga MC, Palma-Dibb RG, Só MV, Matsumoto MA, Faria G, et al. Effect of sodium hypochlorite under several formulations on root canal dentin microhardness. *J Investig Clin Dent* 2013;4:229–32.
- [19] Kaufman AY, Keila S. Hypersensitivity to sodium hypochlorite. *J Endod* 1989;15:224–6.
- [20] Gursoy UK, Bostanci V, Kosger HH. Palatal mucosa necrosis because of accidental sodium hypochlorite injection instead of anaesthetic solution. *Int Endod J* 2006;39:157–61.
- [21] Pashley EL, Birdsong NL, Bowman K, Pashley DH. Cytotoxic effects of NaOCl on vital tissue. *J Endod* 1985;11:525.
- [22] Zehnder M. Root canal irrigants. *J Endod* 2006;32:389–98.
- [23] Gupta H, Kandaswamy D, Manchanda SK, Shourie S. Evaluation of the sealing ability of two sealers after using chlorhexidine as a final irrigant: an in vitro study. *J Conserv Dent* 2013;16:75–8.
- [24] Matinlinna JP, Lung CYK, Tsoi JKH. Silane adhesion mechanism, in dental applications and surface treatments: a review. *Dent Mater* 2018;34:13–28.
- [25] Daood U, Parolia A, Elkezza A, Yiu CK, Abbott P, Matinlinna JP, et al. An in vitro study of a novel quaternary ammonium silane endodontic irrigant. *Dent Mater* 2019;359:1264–78.
- [26] Daood D, Yiu CKY, Burrow MF. Effect of a novel quaternary ammonium silane cavity disinfectant on cariogenic biofilm formation. *Clin Oral Inves* 2019, <http://dx.doi.org/10.1007/s00784-019-02928-7>.
- [27] Daood U, Yiu CK, Burrow MF, Niu LN, Tay FR. Effect of a novel quaternary ammonium silane on dentin protease activities. *J Dent* 2017;58:19–27.
- [28] Daood D, Yiu CKY, Burrow MF, Niu LN, Tay FR. Effect of a novel quaternary ammonium silane cavity disinfectant on durability of resin-dentine bond. *J Dent* 2017;60:77–86.

- [29] Ahlström B, Thompson RA, Edebo L. The effect of hydrocarbon chain length, pH, and temperature on the binding and bactericidal effect of amphiphilic betaine esters on *Salmonella typhimurium*. *APMIS* 1999;107:318–24.
- [30] Isquith AJ, Abbott EA, Walters PA. Surface-bonded antimicrobial activity of an organosilicon quaternary ammonium chloride. *Appl Microbiol* 1972;24:859–63.
- [31] Liu R, Xu Y, Wu D, Sun Y, Gao H, Yuan G. Comparative study on the hydrolysis kinetics of substituted ethoxysilanes by liquid-state ^{29}Si NMR. *J Non Cryst Solids* 2004;343:61–70.
- [32] Inácio AS, Costa GN, Domingues NS, Santos MS, Moreno AJ, Vaz WL. Mitochondrial dysfunction is the focus of quaternary ammonium surfactant toxicity to mammalian epithelial cells. *Antimicrob Agent Chemo* 2013;57:2631–9.
- [33] Gaweda S, Moran MC, Pais AA, Dias RS, Schillen K, Lindman B. Cationic agents for DNA compaction. *J Colloid Interface Sci* 2008;323:75–83.
- [34] Siddiqui WA, Ahad A, Ahsan H. The mystery of BCL2 family: Bcl-2 proteins and apoptosis: an update. *Arch Tox* 2015;89:289–317.
- [35] Cohen AL, Roh JH, Nallapareddy SR, Hook M, Murray BE. Expression of the collagen adhesin ace by *Enterococcus faecalis* strain OG is not repressed by Ers but requires the Ers box. *FEMS Microbiol Lett* 2013;344:18–24.
- [36] Koehne T, Marshall RP, Jeschke A, Kahl-Nieke B, Schinke T, Amling M. Osteopetrosis, osteopetrorickets and hypophosphatemic rickets differentially affect dentin and enamel mineralization. *Bone* 2013;53:25–33.
- [37] Soares LE. Effects of Er: glaser irradiation and manipulation treatments on dentin components, part 1: fourier Transform-Raman study. *J Biomed Opt* 2009;14:1–7.
- [38] Schuster KC, Reese I, Urlaub E, Gapes JR, Lendl B. Multidimensional information on the chemical composition of single bacterial cells by confocal Raman microspectroscopy. *Anal Chem* 2000;72:5529–34.
- [39] Fedorowicz Z, Nasser M, Sequeira P. Irrigants for non-surgical root canal treatment in mature permanent teeth. *Cochrane Database Syst Rev* 2012:CD008948.
- [40] Rodrigues CT, de Andrade FB, de Vasconcelos LRS. Antibacterial properties of silver nanoparticles as a root canal irrigant against *Enterococcus faecalis* biofilm and infected dentinal tubules. *Int Endod J* 2018;51:901–11.
- [41] Zehnder M. Root canal irrigants. *J Endod* 2006;32:389–98.
- [42] Wright PP, Kahler B, Walsh LJ. Alkaline sodium hypochlorite irrigant and its chemical interactions. *Mater (Basel)* 2017;10:1–8.
- [43] Pascon FM, Kantovitz KR, Sacramento PA, et al. Effect of sodium hypochlorite on dentine mechanical properties: a review. *J Dent* 2009;37:903–8.
- [44] Gonçalves LS, Rodrigues RCV, Andrade Junior CV, et al. The effect of sodium hypochlorite and chlorhexidine as irrigant solutions for root canal disinfection: a systematic review of clinical trials. *J Endod* 2016;42:527–32.
- [45] Peters MDJ, Ma Q, Godfrey CM. Guidance for conducting systematic scoping reviews. *Int J Evid Based Health* 2015;13:141–6.
- [46] Nobuhiro T, Bente N. Ecological hypothesis of dentin and root caries. *Caries Res* 2016;50:422–31.
- [47] Figdor D, Sundqvist G. A big role for the very small — understanding the endodontic microbial flora. *Aust Dent J* 2007;52:S38–51.
- [48] Stuart CH, Schwartz SA, Beeson TJ, Owatz CB. *Enterococcus faecalis*: its role in root canal treatment failure and current concepts in retreatment. *J Endod* 2006;2:93–8.
- [49] Teixeira CS, Felipe MCS, Felipe WT. The effect of application time of EDTA and NaOCl on intracanal smear layer removal: an SEM analysis. *Int Endod J* 2005;38:285–90.
- [50] Vivacqua-Gomes N, Ferraz CC, Gomes BP, Zaia AA, Teixeira FB, Souza-Filho FJ. Influence of irrigants on the coronal microleakage of laterally condensed gutta-percha root fillings. *Int Endod J* 2002;35:791–5.
- [51] Niazi SA, Clark D, Do T, Gilbert SC, Foschi F, Mannocci F. The effectiveness of enzymic irrigation in removing a nutrient-stressed endodontic multispecies biofilm. *Int Endod J* 2014;47:756–68.
- [52] Minghua Yu, Gu Guotuan, Meng Wei-Dong, Qing Feng-Ling. Superhydrophobic cotton fabric coating based on a complex layer of silica nanoparticles and perfluorooctylated quaternary ammonium silane coupling agent. *Appl Sur Sci* 2007;253:3669–73.
- [53] Inoue N, Tsujimoto A, Takimoto M, Ootsuka E, Endo H, Takamizawa T. Surface free-energy measurements as indicators of the bonding characteristics of single step self-etching adhesives. *Eur J Oral Sci* 2010;118:525–30.
- [54] Chen X, Wang Z, Duan N, Zhu G, Schwarz E, Xie C. Osteoblast-osteoclast interactions. *Connect Tissue Res* 2017;3:1–9.
- [55] Josse J, Velard F, Gangloff SC. *Staphylococcus aureus* vs. osteoblast: relationship and consequences in osteomyelitis. *Front Cell Infect Microbiol* 2015;4:85.
- [56] Patrick K, Reinhard N, Natalia P. On the origin of the band at around 730 cm^{-1} in SERS spectra of Bacteria: stable isotope approach. *Analyst* 2016;141:2874–8.
- [57] Toyama A, Hanada N, Abe Y, Takeuchi H, Harada I. Assignment of adenine ring in-plane vibrations in adenosine on the basis of ^{15}N and ^{13}C isotopic frequency shifts and TUV resonance Raman enhancement. *J Raman Spectrosc* 1994;25:623–30.
- [58] Premasiri WR, Moir DT, Klempner MS, Krieger N, Jones G, Ziegler LD. Characterization of the surface enhanced raman scattering (SERS) of bacteria. *J Phys Chem B* 2005;109:312–20.
- [59] Wiercigroch E, Szafranec E, Czamara K, Pacia MZ, Majzner K, Kochan K, et al. Raman and infrared spectroscopy of carbohydrates: a review. *Spectrochim Acta A Mol Biomol Spectrosc* 2017;185:317–35.
- [60] Lopez-Ochoa J, Montes-García JF, Vázquez C. Gallibacterium elongation factor-Tu possesses amyloid-like protein characteristics, participates in cell adhesion, and is present in biofilms. *J. Micro* 2017;55:745–52.
- [61] Spencer P, Ye Q, Misra A, Goncalves SEP, Laurence JS. Proteins, pathogens and failure at the composite-tooth interface. *J Dent Res* 2014;93:1243–9.
- [62] Devinsky F, Masarova L, Lacko I, Mlynarcik D. Structure activity relationships of soft quaternary ammonium amphiphiles. *Aust J Biol Sci* 1991;2:1–10.
- [63] Nazari A, Bajaj D, Zhang D, Romberg E, Arola D. Aging and the reduction in fracture toughness of human dentin. *J Mech Behav Biomed Mater* 2009;2:550–9.
- [64] Collins MJ, Nielsen-Marsh CM, Hiller J, Smith CI, Roberts JP, Prigodich RV, et al. The survival of organic matter in bone: a review. *Archaeometry* 2002;44:383–94.
- [65] Fengzhi J, Heinrich H, Jonathon H, Müller Daniel J. Assembly of collagen into micro ribbons: effects of pH and electrolytes. *J Struct Biol* 2004;5:268–78.
- [66] Rossi-Fedele G, Guastalli AR, Dogramaci EJ, Steier L, De Figueiredo JA. Influence of pH changes on chlorine-containing endodontic irrigating solutions. *Int Endod J* 2011;44:792–9.
- [67] Jungbluth H, Marending M, De-Deus G, Sener B, Zehnder M. Stabilizing sodium hypochlorite at high pH: effects on soft tissue and dentin. *J Endod* 2011;37:693–6.
- [68] Damen JJM, Ten Cate JM. The effect of silicic acid on calcium phosphate precipitation. *J Dent Res* 1989;68:1355–9.

- [69] Dong Z, Chang J, Deng Y, Joiner A. Tricalcium silicate induced mineralization for occlusion of dentinal tubules. *Aust Dent J* 2011;56:175–80.
- [70] Ma J, Tong Z, Ling J, Liu H, Wei X. The effects of sodium hypochlorite and chlorhexidine irrigants on the antibacterial activities of alkaline media against *Enterococcus faecalis*. *Arch Oral Bio* 2015;7:1075–81.
- [71] Luddin N, Mohamed Aly Ahmed H. The antibacterial activity of sodium hypochlorite and chlorhexidine against *Enterococcus faecalis*: a review on agar diffusion and direct contact methods. *J Conserv Dent* 2013;1:9–16.
- [72] Choi G, Jeong GM, Oh MS, Joo M, Im SG, Jeong KJ. Robust thin film surface with a selective antibacterial property enabled via a cross-linked ionic polymer coating for infection-resistant medical applications. *ACS Biomater Sci Eng* 2018;7:2614–22.
- [73] Roter Marins JS, Sassone LM, Fidel SR, Ribeiro DA. In vitro genotoxicity and cytotoxicity in murine fibroblasts exposed to EDTA, NaOCl, MTAD and citric acid. *Braz Dent J* 2012;23:527–33.
- [74] Mancheno-Posso P, Dittler RF, Lewis D, Juang P, XY JI, Xu XH, Lynch DC. Review of status, trends, and challenges in working with silane and functional silanes. In: Moriguchi K, Utagawa SS, editors. *Silane, chemistry, applications and performance*. New York: Nova Science Publishers; 2013. p. 66–87.
- [75] Al-Ahmad A, Ameen H, Pelz K. Antibiotic resistance and capacity for biofilm formation of different bacteria isolated from endodontic infections associated with root-filled teeth. *J Endod* 2014;40:223–30.
- [76] Li Y, Kuan Y, Lee S, Huang F. Cytotoxicity and genotoxicity of chlorhexidine on macrophages in vitro. *Environ Toxicol* 2014;29:452–8.
- [77] Giuseppina N, Hany Mohamed AA, Giuseppe Ettore M, Cinzia C, Gianluca G, Sandro R, et al. Chromographic analysis and cytotoxic effects of chlorhexidine and sodium hypochlorite reaction mixtures. *J Endo* 2017;43:1545–52.
- [78] Tu YY, Yang CY, Chen RS. Effects of chlorhexidine on stem cells from exfoliated deciduous teeth. *J Formos Med Assoc* 2015;114:17–22.
- [79] Chawner JA, Gilbert P. Interaction of the bisbiguanides chlorhexidine and alexidine with phospholipid vesicles: evidence for separate modes of action. *J Appl Microbiol* 1989;66:253–8.
- [80] Huang X, Zhang J, Huang C. Effect of intracanal dentine wettability on human dental pulp cell attachment. *Int Endod J* 2012;45:346–53.
- [81] Liolios E, Economides N, Parissis-Messimeris S, Boutsoukis A. The effectiveness of three irrigating solutions on root canal cleaning after hand and mechanical preparation. *Int Endod J* 1997;30:51–7.
- [82] Basset J, Mendham J. *Vogel - Análise química quantitativa*. 6rd ed. Rio de Janeiro: LTC; 2002. p. 462.